Dephasing effects and shot noise in quantum Hall wires: Green's function formalism

Alessandro Cresti[1] and Giuseppe Pastori Parravicini[2]
[1]*NEST-CNR-INFM and Dipartimento di Fisica "E. Fermi," Università di Pisa, Largo Pontecorvo 3, I-56127 Pisa, Italy and CEA, LETI-Minatec, 17 rue des Martyrs, 38054 Grenoble Cedex 9, France*
[2]*NEST-CNR-INFM and Dipartimento di Fisica "A. Volta," Università di Pavia, Via A. Bassi 6, I-27100 Pavia, Italy*
(Received 10 April 2008; revised manuscript received 30 July 2008; published 18 September 2008)

We study the effects of many-body dephasing processes on the electron conductance and current fluctuations of quantum wires, with particular attention to Hall bars. The theoretical study is based on the nonequilibrium Green's function formalism and the self-consistent Born approximation for the dephasing self-energy operators. The numerical study of the retarded and lesser Green's functions of the interacting system is carried out by means of continued fractions and iterative techniques, within a tight-binding description of the electronic device. The crossover from the noise regime to the noiseless regime with its striking universal features emerges with great evidence from the calculated behavior of conductance and shot noise in the studied quantum wires.

DOI: 10.1103/PhysRevB.78.115313 PACS number(s): 73.63.Nm, 72.70.+m

I. INTRODUCTION

Quantum transport in low-dimensional systems in the presence of scattering mechanisms is the subject of intense investigations, motivated by the desire of deeper comprehension and improved control of the carrier flow in mesoscopic devices. Elastic and inelastic scattering processes are of much interest to characterize transport phenomena in a variety of nanoscale systems, including molecular junctions and molecular motors,[1–4] graphite-like materials,[5–8] organic and inorganic nanostructures,[9–12] spintronics and magnetoelectronics devices,[13,14] quantum Hall wires and magnetotransport.[15–19] In particular, in quantum Hall wires, conductance fluctuations and dephasing processes have been described numerically and mimicked phenomenologically with fictitious probes carrying zero net current and in contact with fictitious reservoirs.[15–17]

The aim of this paper is to elaborate a theoretical and numerical procedure for a unified description of noise and noiseless regimes in quantum Hall wires, and a clear crossover from the dissipative to the dissipationless current flow. This requires a rigorous formulation of the many-body problem from one side, and the possibility of solving the transport equations with highest numerical accuracy from the other side. This in order to account for both the sample dependent features and the universal aspects of magnetotransport on the same footing. In particular, it is well known that the observed plateaus of the Hall resistance in the integer Hall effect entail values of the von Klitzing constant[20] reproducible to better than eight significant digits independently of the semiconductor used, shape and size of the sample, disorder and imperfections, impurity or alloys fluctuations, and other dephasing processes envisaged to occur in any experimental device.[21] Then, to tackle the problem of magnetotransport and dephasing in quantum wires, the formal and numerical apparatus should be capable of such an accuracy.

For an *ab initio* study of elastic and inelastic processes in mesoscopic systems, the main tool is represented by the nonequilibrium Keldysh Green's function formalism,[22–25] which encompasses the full many-body theory. In this formalism, the presence of many-body interactions (such as electron-electron, electron-phonon, ensemble averages of disorder fluctuations, dephasing effects) can be described by an appropriate fourfold set of self-energy operators $\Sigma^{R,A,<,>(\mathrm{scatt})}$ (retarded, advanced, lesser and greater). Quantum transport is then studied by solving the Keldysh kinetic equations for the retarded and advanced propagators, and for the lesser and greater correlation functions.

The self-energy operators of the actual scattering mechanism can be calculated at various degrees of approximation, depending on the scattering processes at work. The many-body diagrammatic perturbation series is often handled within the self-consistent Born approximation.[25–29] This approach rigorously fulfills the key condition of current conservation, and yet the whole apparatus remains manageable enough for high accuracy numerical calculations of transport properties. In fact, in the Born approximation, the self-energy operators of the scattering processes are linear functionals of the Green's functions. By virtue of linearity, we show how to elaborate the dephasing effects rigorously by means of a mixing of continued fraction expansion[29–31] and linear homogeneous equations.

In Sec. II, we consider the tight-binding microscopic description of the electronic gas in the two-dimensional quantum wire and the many-body model of dephasing within the self-consistent Born approximation. In Sec. III, convenient expressions of the full set of retarded, advanced, lesser and greater Green's functions and self-energy operators for scattering are reported. In Secs. IV and V, the expressions of the average current and the current fluctuations are provided for quantum wires in the presence of dephasing effects. Although the attention of our work is focused on quantum wires, the presented formalism is quite general and transferable to other two-dimensional systems. Section VI reports the numerical simulations of transport in quantum wires, both in the absence and in the presence of magnetic fields. It is shown that in the absence of magnetic fields, the dephasing entails shot noise and dissipative flow at any chosen Fermi energy, even in ideally clean structures. On the contrary, in the presence of strong magnetic fields, noise and noiseless regimes are observed in the same sample at different energies. The crossover from the former to the latter regime is signaled by the spectacular emergence of conduc-

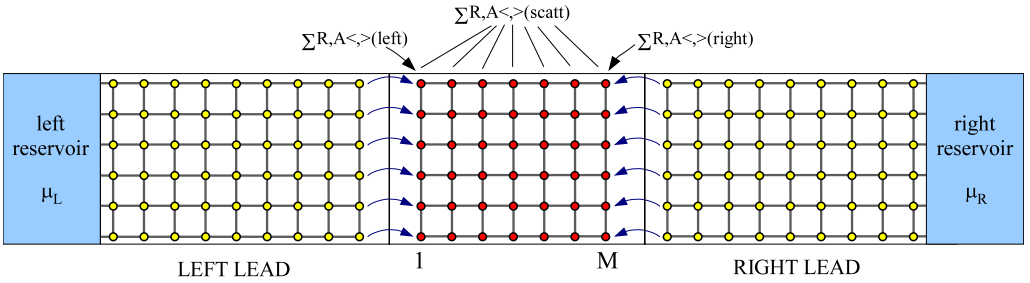

FIG. 1. (Color online) Schematic setup of a quantum wire for the analysis of electron transport. The central region, where phase-breaking effects are active, extends from column 1 to column M ($M \geq 1$) and embodies a total of MN sites. Scattering operators $\Sigma^{R,A,\langle,\rangle(\mathrm{scatt})}$ are confined to the central device. The effect of the left and right open leads on the central region is expressed by $\Sigma^{R,A,\langle,\rangle(\mathrm{left})}$ and $\Sigma^{R,A,\langle,\rangle(\mathrm{right})}$, confined to column 1 and column M, respectively.

tance quantization and vanishing of shot noise. Section VII contains the conclusions.

II. TIGHT-BINDING ELECTRON HAMILTONIAN AND DEPHASING MODEL IN QUANTUM WIRES

For the theoretical treatment of the two-dimensional electron gas in quantum wires in the presence of phase-breaking processes, we adopt a tight-binding electronic Hamiltonian and describe dephasing effects within the self-consistent Born approximation. The two-dimensional quantum wire under attention is infinitely extended along the longitudinal direction and has finite width in the transverse direction. The tight-binding Hamiltonian is mapped on a square lattice topology[32–34] with a single orbital per site and nearest-neighbor interactions only. The structure is conceptually split into three parts: the left lead, the right lead, and the central part coupled to them. We assume that some kind of dephasing mechanism is active among the carriers of the two-dimensional electron gas in the central part of the device, while the leads are free from scattering. According to the nonequilibrium Keldysh theory, the many-body interactions can be described by appropriate self-energy operators of the type $\Sigma^{R,A,\langle,\rangle(\mathrm{scatt})}$, whose matrix elements are nonvanishing only within the sites of the central device, regardless of the nature and the origin of the scattering processes at work. As usual, the effects of open leads on the orbitals of the central device are described by the corresponding self-energy operators $\Sigma^{R,A,\langle,\rangle(\mathrm{leads})}$. A scheme of the device is shown in Fig. 1.

We specify some notations of frequent use in the following. In general the matrix element of a Green's function operator (say the retarded operator G^R) carries four lower labels $G^R_{mn,m'n'}(E)$: This is required to specify the propagator from site $m'n'$ to the site mn. The abridged notation with only two labels, for instance $G^R_{mm'}(E)$, is used to denote the propagator from a site (not yet specified) of column m' to a site (not yet specified) of column m. The rank of such a matrix is thus N, and corresponds to the transverse degrees of freedom. In the study of the Keldysh kinetic equations, the interest is often confined to the MN degrees of freedom of the central device. In these cases, we indicate the sites with a single label. As an example, we adopt the notation $G^R_{ij}(E)$ ($i,j \in$ central device) to denote the matrix element of the retarded Green's functions between the sites i and j of the central device. The notation adopted each time is apparent from the context.

Let us consider the description of dephasing processes in the central device. Within the Keldysh formalism, elastic or inelastic scattering mechanisms can be accounted for by self-energy operators obtained by diagrammatic techniques. We adopt the self-consistent Born approximation to picture many-body interactions. This approximation has several advantages: (i) it entails a partial summation of the infinite terms of the diagrammatic perturbative series, (ii) it rigorously fulfills the key condition of current conservation in stationary regime, (iii) it expresses the self-energy operators as linear functionals of the Green's function itself, and (iv) thanks to linearity, it is particularly suitable for the application of the highly effective iterative procedures.

The above considerations can be put on a rigorous quantitative basis by elaborating the general *ab initio* formulation of the electron transport in mesoscopic devices in the presence of vibrational effects and other many-body interactions, along the lines of Ref. 25. Many-body interactions, in agreement with the Keldysh nonequilibrium formalism, are expressed (at least in principle) by advanced, retarded, lesser and greater self-energy operators. Within the self-consistent Born approximation, the self-energy operators for dephasing are related to the electron Green's functions by an appealing linear form. Furthermore, for dephasing models that are local in energy and space,[25–29] the functional relation between scattering operators and electron propagators takes the diagonal form

$$\Sigma^{R,A,\langle,\rangle(\mathrm{scatt})}_{ij}(E) = \gamma^2_{ii}\delta_{ij}G^{R,A,\langle,\rangle}_{ij}(E) \quad (i,j = 1,2,\ldots,MN), \tag{1}$$

where i,j denote sites of the central device, and γ_{ii} are positive parameters with the dimension of energy, which express the effective coupling between the fluctuating field and the fermion field. For the sake of simplicity, these parameters are taken as independent of the site, i.e., $\gamma_{ii}=\gamma$ (the case of site dependent γ_{ii} can be treated similarly). The local dephasing model (1) describes simultaneous phase and momentum relaxation. It has been widely exploited in the literature[23–29] for the study, e.g., of alloy disorder effects, interface roughness, impurities ensemble averages, phonon dephasing and others. Equation (1) can be written in the compact form

$$\Sigma^{R,A,<,>(\mathrm{scatt})}(E) = \gamma^2 \mathcal{D}_{\mathrm{sup}} G^{R,A,<,>}(E) \quad (\mathrm{sites} \in \mathrm{central\ device}), \tag{2}$$

where $\mathcal{D}_{\mathrm{sup}}$ is a "superoperator" that preserves the diagonal elements of the given matrix on which it acts, while setting to zero all the off-diagonal elements. Within the stated formalism, we can now investigate the phase-breaking effects on conductance and shot noise in quantum wires, in the absence or in the presence of external magnetic fields.

III. GREEN'S FUNCTIONS AND SELF-ENERGY OPERATORS FOR DEPHASING DISORDER

In this section, we propose a formal elaboration (suitable for computational implementation) of the electronic Green's functions and scattering operators in the central structure, since they are the main ingredients for investigating the transport properties of the system. To this aim, we proceed in two stages: (i) the calculation of the retarded (and advanced) propagators by means of a convenient continued fraction expansion of the propagators, and (ii) the solution of the kinetic equations that control the lesser and greater Green's functions, by means of linear nonhomogeneous equations. Throughout the whole section, it is understood that any matrix has rank equal to the number of degrees of freedom of the central region (even when the rank is not explicitly specified).

Let us consider the equations for the retarded Green's function in the presence of dephasing on the M columns of the device central region. Within the self-consistent Born approximation, the retarded Green's function in the central device becomes

$$G^R(E) = \frac{1}{E - H^{(C)} - \Sigma^{R(\mathrm{leads})}(E) - \Sigma^{R(\mathrm{scatt})}(E)} \quad (\mathrm{sites} \in \mathrm{central\ device}), \tag{3a}$$

where $H^{(C)}$ is the electronic Hamiltonian of the central device, $\Sigma^{R(\mathrm{leads})}$ is the retarded self-energy due to the left and right open leads, and

$$\Sigma^{R(\mathrm{scatt})}(E) = \gamma^2 \mathcal{D}_{\mathrm{sup}} G^R(E) \quad (\mathrm{sites} \in \mathrm{central\ device}) \tag{3b}$$

is the retarded self-energy within the adopted Born approximation. The solution of the above coupled equations is given by the continued fraction

$$G^R(E) = \frac{1}{E - H^{(C)} - \Sigma^{R(\mathrm{leads})} - \gamma^2 \mathcal{D}_{\mathrm{sup}} \frac{1}{E - H^{(C)} - \Sigma^{R(\mathrm{leads})} - \gamma^2 \mathcal{D}_{\mathrm{sup}} \frac{1}{E - \ldots}}}. \tag{4}$$

By calculating the above expression, we obtain the retarded Green's function on the central device, and hence the scattering retarded self-energies according to Eq. (3b). As reported in the literature,[23,29] the matrix continued fractions of type (4) are found to be well satisfactory for convergence purposes. This in analogy to the well-established fact that scalar continued fractions are generally characterized by a very fast convergence to the fixed point value.[30,31] In summary, the very accurate calculation of the retarded Green's function (4) owes much to the fast convergence of the continued fraction expansion, and to the well-established renormalization-decimation techniques[31–34] for the calculations of the matrices entering therein.

Once the retarded (and advanced) Green's functions of the central region are available, the expression of the lesser (or greater) Green's function can be obtained by the standard kinetic equation

$$G^< = G^R \Sigma^{<(\mathrm{leads})} G^A + G^R \Sigma^{<(\mathrm{scatt})} G^A \quad (\mathrm{sites} \in \mathrm{central\ device}), \tag{5}$$

together with Eq. (2). The result is

$$\Sigma^{<(\mathrm{scatt})}(E) = \gamma^2 \mathcal{D}_{\mathrm{sup}} [G^R \Sigma^{<(\mathrm{leads})} G^A + G^R \Sigma^{<(\mathrm{scatt})} G^A]. \tag{6}$$

We notice that

$$\Sigma^{<(\mathrm{leads})}(E) = i\, f_L \Gamma^{(\mathrm{left})}(E) + i\, f_R \Gamma^{(\mathrm{right})}(E), \tag{7}$$

where

$$\Gamma^{(\mathrm{left})} = i\Sigma^{R(\mathrm{left})} - i\Sigma^{A(\mathrm{left})}, \quad \Gamma^{(\mathrm{right})} = i\Sigma^{R(\mathrm{right})} - i\Sigma^{A(\mathrm{right})} \tag{8}$$

are the linewidth operators, which couple the central device to the left and right leads, respectively; $f_L(E)$ and $f_R(E)$ are the Fermi-Dirac distribution functions of the left and right reservoirs. From Eqs. (6) and (7) one obtains

$$\Sigma^{<(\mathrm{scatt})}(E) = i\, f_L K^{(\mathrm{left})}(E) + i\, f_R K^{(\mathrm{right})}(E), \tag{9}$$

where

$$K^{(\mathrm{left})}(E) = \gamma^2 \mathcal{D}_{\mathrm{sup}} [G^R \Gamma^{(\mathrm{left})} G^A + G^R K^{(\mathrm{left})} G^A], \tag{10a}$$

$$K^{(\mathrm{right})}(E) = \gamma^2 \mathcal{D}_{\mathrm{sup}} [G^R \Gamma^{(\mathrm{right})} G^A + G^R K^{(\mathrm{right})} G^A]. \tag{10b}$$

Similar to $\Sigma^{R,A,<,>(\mathrm{scatt})}$, also $K^{(\mathrm{left})}$ and $K^{(\mathrm{right})}$ are diagonal matrices, defined exclusively on the sites of the central device. The K matrices have a clear physical meaning: They represent the effective coupling of the central device to the left and right reservoirs, mediated by the scattering events.

We can solve Eq. (9) explicitly by exploiting their linear structure. Let us define a matrix P and a matrix Q (both of rank equal to the number of degrees of freedom of the central device) as follows:

$$P_{j\nu} = G^R_{j\nu} G^A_{\nu j} \equiv |G^R_{j\nu}|^2; \quad Q = \frac{1}{1 - \gamma^2 P}.$$

The elements of the P matrix, between any two sites of the central region, are defined as the product of the retarded and advanced propagators back and forth between the chosen sites. The matrix Q is the inverse of $1 - \gamma^2 P$. Equations (10a) and (10b) can be recast in the form

$$K^{(\mathrm{left})}_{jj}(E) = \gamma^2 [G^R \Gamma^{(\mathrm{left})} G^A]_{jj} + \gamma^2 \sum_{\nu} P_{j\nu} K^{(\mathrm{left})}_{\nu j},$$

then the expression for the $K^{(\mathrm{left/right})}$ matrix elements reads

$$K_{jj}^{(\mathrm{left})} = \gamma^2 \sum_{\nu} Q_{j\nu}[G^R \Gamma^{(\mathrm{left})} G^A]_{\nu\nu},$$

$$K_{jj}^{(\mathrm{right})} = \gamma^2 \sum_{\nu} Q_{j\nu}[G^R \Gamma^{(\mathrm{right})} G^A]_{\nu\nu}. \tag{11}$$

This is the exact and reasonably simple expression of the K matrices, which play a role formally similar to the leads $\Gamma^{(\mathrm{left/right})}$ matrices, as evident from comparison of Eq. (7) and Eq. (9).

Before closing this section, it is worthwhile to establish a key identity that strongly simplifies the calculation of shot noise in devices with many-body effects on the central region. Within the central device and in the presence of scattering events, it holds

$$G^R - G^A = (-i)[G^R \Gamma^{(\mathrm{left})} G^A + G^R \Gamma^{(\mathrm{right})} G^A + G^R \Gamma^{(\mathrm{scatt})} G^A], \tag{12}$$

with

$$\Gamma^{(\mathrm{scatt})} = i\Sigma^{R(\mathrm{scatt})} - i\Sigma^{A(\mathrm{scatt})}.$$

By multiplying Eq. (12) by $(+i)\gamma^2$, applying the superoperator $\mathcal{D}_{\mathrm{sup}}$, to both members, and using the basic properties of the self-consistent Born approximation, we obtain

$$\Gamma^{(\mathrm{scatt})} = \gamma^2 \mathcal{D}_{\mathrm{sup}}[G^R \Gamma^{(\mathrm{left})} G^A + G^R \Gamma^{(\mathrm{right})} G^A + G^R \Gamma^{(\mathrm{scatt})} G^A]. \tag{13}$$

We solve this equation by means of the Q-matrix technique adopted for Eqs. (10a) and (10b), and obtain the identity

$$K^{(\mathrm{left})} + K^{(\mathrm{right})} \equiv \Gamma^{(\mathrm{scatt})}. \tag{14}$$

We now have all the ingredients for the calculation of the average current and current fluctuations in mesoscopic devices in the presence of dephasing effects.

IV. CURRENTS IN QUANTUM WIRES IN THE PRESENCE OF DEPHASING EFFECTS

With the results of Sec. III we can discuss dephasing effects on the electronic conductance of two-dimensional mesoscopic systems. The attention of the present paper is focused on quantum wires represented on a square-lattice topology with nearest-neighbor interactions. However, the underlying formalism is general and ready (with minor modifications) to handle other mesoscopic systems described by a variety of tight-binding model Hamiltonians, including composite lattice topologies and spin degrees of freedom.

Consider the quantum wire schematically represented in Fig. 1. According to the nonequilibrium Green's function formalism, the average current through the device is given by the expression

$$I = \frac{-2e}{\hbar} \int \frac{dE}{2\pi} \mathrm{Tr}[\Sigma_{11}^{<(\mathrm{left})} G_{11}^{>} - \Sigma_{11}^{>(\mathrm{left})} G_{11}^{<}] \quad (i,j = 1,2,\ldots,N), \tag{15}$$

where the factor 2 takes into account the spin degeneracy. The matrices in Eq. (15) are understood as the block part corresponding to the Hilbert space of column 1, and have thus rank N. What is remarkable of Eq. (15) is its general validity, regardless of the presence or not of many-body effects in the central region, as can be established by revisiting the procedures for its elaboration.

The expressions for the lesser (and greater) self-energies of the left lead on the sites of column 1 are

$$\Sigma_{11}^{<(\mathrm{left})} = i f_L \Gamma_{11}^{(\mathrm{left})}; \quad \Sigma_{11}^{>(\mathrm{left})} = -i(1-f_L)\Gamma_{11}^{(\mathrm{left})}. \tag{16a}$$

Once specified for the quantities entering Eq. (15), Eqs. (5), (7), and (9) for the lesser (and greater) Green's functions give

$$G_{11}^{<} = +i f_L G_{11}^R \Gamma_{11}^{(\mathrm{left})} G_{11}^A + i f_L [G^R K^{(\mathrm{left})} G^A]_{11} + i f_R G_{1N}^R \Gamma_{NN}^{(\mathrm{right})} G_{N1}^A + i f_R [G^R K^{(\mathrm{right})} G^A]_{11}, \tag{16b}$$

$$G_{11}^{>} = -i(1-f_L) G_{11}^R \Gamma_{11}^{(\mathrm{left})} G_{11}^A - i(1-f_L) G^R K^{(\mathrm{left})} G_{11}^A - i(1-f_R) G_{1N}^R \Gamma_{NN}^{(\mathrm{right})} G_{N1}^A - i(1-f_R)[G^R K^{(\mathrm{right})} G^A]_{11}. \tag{16c}$$

By inserting Eqs. (16a)–(16c) into expression (15), the average current through the device takes the form

$$I_{\mathrm{tot}} = I_{\mathrm{coh}} + I_{\mathrm{inc}}, \tag{17a}$$

$$I_{\mathrm{coh}} = \frac{-2e}{\hbar} \int \frac{dE}{2\pi} (f_L - f_R) \mathrm{Tr}[\Gamma_{11}^{(\mathrm{left})} G_{1N}^R \Gamma_{NN}^{(\mathrm{right})} G_{N1}^A], \tag{17b}$$

$$I_{\mathrm{inc}} = \frac{-2e}{\hbar} \int \frac{dE}{2\pi} (f_L - f_R) \mathrm{Tr}[\Gamma_{11}^{(\mathrm{left})} (G^R K^{(\mathrm{right})} G^A)_{11}]. \tag{17c}$$

From the above equations, we obtain the coherent, incoherent, and total transmission matrices

$$T_{\mathrm{coh}}(E) = \Gamma_{11}^{(\mathrm{left})} G_{1N}^R \Gamma_{NN}^{(\mathrm{right})} G_{N1}^A, \tag{18a}$$

$$T_{\mathrm{inc}}(E) = \Gamma_{11}^{(\mathrm{left})} [G^R K^{(\mathrm{right})} G^A]_{11}, \tag{18b}$$

$$T_{\mathrm{tot}}(E) = T_{\mathrm{coh}}(E) + T_{\mathrm{inc}}(E). \tag{18c}$$

The differential conductance and its coherent and incoherent components are given by the expression

$$\sigma_{\mathrm{tot,coh,inc}}(E) = \frac{2e^2}{h} \mathrm{Tr}[T_{\mathrm{tot,coh,inc}}(E)]. \tag{19}$$

From the above results, it is seen that the total current and total conductance through the device can be split into a coherent and an incoherent contribution. The former corresponds to carriers crossing the sample with no assistance of scattering events; the latter corresponds to carriers crossing the sample subjected to one or more scattering processes.

This splitting of the current into two components, its theoretical foundation and importance for interpretative purposes need a few comments. First of all, it is well known that the self-consistent Born approximation of many-body inter-

actions automatically satisfies the key requirement of total current conservation (i.e., conservation of $I_{\rm tot}=I_{\rm coh}+I_{\rm inc}$). To be specific, this means that the total current injected or extracted from the left lead to the central device [given by Eq. (15)] equals the total current extracted or injected from the right lead to the central device (given by a corresponding equation). For the sake of completeness, after lengthy derivations, we have verified that both coherent and incoherent components are separately conserved, in spite of the asymmetry of the incoherent contribution with respect to the left and right indexes.

We also wish to notice that, of course, any specific experimental measurement of current concerns the total current, and cannot discern between coherent and incoherent components. However, the understanding of the behavior of total current versus relevant parameters (i.e., length of the system, strength of the many-body coupling, microscopic model of interaction, crossover between different transport regimes, etc.) cannot be pursued or predicted without the theoretical splitting of the current into its incoherent and coherent components.

V. CURRENT FLUCTUATIONS IN QUANTUM WIRES IN THE PRESENCE OF DEPHASING EFFECTS

We consider now the calculation of the current fluctuations. Within the Keldysh formalism, the quantum statistical average of the current-current correlation function can be performed by means of the Wick theorem applied in a region free from scattering processes (in the leads, for instance between column 0 and column 1). The spectral density of noise in the zero-frequency limit is given by the Zhu-Balatsky expression[35]

$$S_{01}(0)=\frac{2e^2}{\hbar}\int\frac{dE}{2\pi}\mathrm{Tr}\,F(E), \tag{20a}$$

where

$$\begin{aligned}F(E)=&-f_L(1-f_L)[\Gamma_{11}^{(\rm left)}G_{11}^R\Gamma_{11}^{(\rm left)}G_{11}^R+\Gamma_{11}^{(\rm left)}G_{11}^A\Gamma_{11}^{(\rm left)}G_{11}^A]\\&+if_L\Gamma_{11}^{(\rm left)}G_{11}^{>}-i(1-f_L)\Gamma_{11}^{(\rm left)}G_{11}^{<}+\Gamma_{11}^{(\rm left)}G_{11}^{<}\Gamma_{11}^{(\rm left)}G_{11}^{>}\\&+f_L\Gamma_{11}^{(\rm left)}(G_{11}^R-G_{11}^A)\Gamma_{11}^{(\rm left)}G_{11}^{>}-(1-f_L)\\&\times\Gamma_{11}^{(\rm left)}G_{11}^{<}\Gamma_{11}^{(\rm left)}(G_{11}^R-G_{11}^A).\end{aligned} \tag{20b}$$

The matrices in Eqs. (20a) and (20b) are restricted in the first column subspace and have rank N. The above equation provides the general exact result for the noise power of the current fluctuations in a two-terminal conductor: It includes both shot and thermal noise. Remarkably, Eqs. (20a) and (20b) are valid even in the presence of many-body interactions in the central region.

The purpose of this section is to analyze and elaborate the Zhu-Balatsky formula[35] in order to describe the current noise quantitatively. In fact, the pieces of information on the transport regimes (for instance, dissipative or dissipationless regime in quantum Hall wires) provided by the study of shot noise and Fano factor are valuable and complementary to the ones provided by the study of average current and conductance quantization.

In a two-terminal device, expressions (20a) and (20b) can be decomposed in the general form

$$\begin{aligned}F(E)=&f_L(1-f_L)A_{LL}+f_L(1-f_R)A_{LR}+f_R(1-f_L)A_{RL}\\&+f_R(1-f_R)A_{RR}.\end{aligned} \tag{21}$$

In the case $\mu_L<\mu_R$, and the temperature is zero, the shot noise is determined by the term of the type $f_R(1-f_L)A_{RL}$, and can be calculated as follows. Using Eqs. (16a)–(16c) for $G_{11}^{\langle\rangle}$, it is seen by inspection that the terms in Eqs. (20a) and (20b) that give rise to the product $f_R(1-f_L)$ are three, namely,

$$A_{RL}^{(1)}\Rightarrow -i(1-f_L)\Gamma_{11}^{(\rm left)}G_{11}^{<},$$

$$A_{RL}^{(2)}\Rightarrow \Gamma_{11}^{(\rm left)}G_{11}^{<}\Gamma_{11}^{(\rm left)}G_{11}^{>},$$

$$A_{RL}^{(3)}\Rightarrow -(1-f_L)\Gamma_{11}^{(\rm left)}G_{11}^{<}\Gamma_{11}^{(\rm left)}(G_{11}^R-G_{11}^A).$$

By using Eq. (12) and Eqs. (16a)–(16c) (and leaving implicit the trace operation on the orbitals of the first column, for notation simplicity), the expressions of the three terms become

$$\begin{aligned}A_{RL}^{(1)}=&\Gamma_{11}^{(\rm left)}G_{1N}^R\Gamma_{NN}^{(\rm right)}G_{N1}^A+\Gamma_{11}^{(\rm left)}[G^RK^{(\rm right)}G^A]_{11}\\\equiv&T_{\rm coh}+T_{\rm inc}\equiv T_{\rm tot},\end{aligned}$$

$$\begin{aligned}A_{RL}^{(2)}=&[\Gamma_{11}^{(\rm left)}G_{1N}^R\Gamma_{NN}^{(\rm right)}G_{N1}^A+\Gamma_{11}^{(\rm left)}(G^RK^{(\rm right)}G^A)_{11}]\\&\times[\Gamma_{11}^{(\rm left)}G_{11}^R\Gamma_{11}^{(\rm left)}G_{11}^A+\Gamma_{11}^{(\rm left)}(G^RK^{(\rm left)}G^A)_{11}]\\=&T_{\rm tot}\times[\Gamma_{11}^{(\rm left)}G_{11}^R\Gamma_{11}^{(\rm left)}G_{11}^A+\Gamma_{11}^{(\rm left)}(G^RK^{(\rm left)}G^A)_{11}],\end{aligned}$$

$$\begin{aligned}A_{RL}^{(3)}=&-\Gamma_{11}^{(\rm left)}[G_{1N}^R\Gamma_{NN}^{(\rm right)}G_{N1}^A+(G^RK^{(\rm right)}G^A)_{11}]\\&\times\Gamma_{11}^{(\rm left)}[G_{11}^R\Gamma_{11}^{(\rm left)}G_{11}^A+G_{1N}^R\Gamma_{NN}^{(\rm right)}G_{N1}^A\\&+(G^R\Gamma^{(\rm scatt)}G^A)_{11}]\\=&-T_{\rm tot}[\Gamma_{11}^{(\rm left)}G_{11}^R\Gamma_{11}^{(\rm left)}G_{11}^A+T_{\rm coh}\\&+\Gamma_{11}^{(\rm left)}(G^R\Gamma^{(\rm scatt)}G^A)_{11}].\end{aligned}$$

By summing up the three contributions we obtain the following expression for the shot-noise coefficient:

$$\begin{aligned}A_{RL}(E)=&T_{\rm tot}+T_{\rm tot}\Gamma_{11}^{(\rm left)}[G^RK^{(\rm left)}G^A]_{11}\\&-T_{\rm tot}T_{\rm coh}-T_{\rm tot}\Gamma_{11}^{(\rm left)}[G^R\Gamma^{(\rm scatt)}G^A]_{11}\\=&T_{\rm tot}-T_{\rm tot}T_{\rm coh}-T_{\rm tot}\Gamma_{11}^{(\rm left)}[G^RK^{(\rm right)}G^A]_{11}\\\equiv&T_{\rm tot}-T_{\rm tot}^2,\end{aligned} \tag{22}$$

where we exploited identity (14).

The basic formal structure of the shot noise, demonstrated for the adopted dephasing model and summarized by Eq. (22), is suitable for both computational purpose and general considerations. The main message of Eq. (22) is that the noise for interacting electrons in the adopted model is sub-Poissonian, since it has the same formal expression of a "fictitious" system of noninteracting electrons. For genuinely

noninteracting electrons, the expression of the transmission matrix only involves the standard coherent component. For interacting electrons the transmission matrix of interest is inclusive of both the coherent and incoherent terms. It is also evident that the zero-temperature shot noise is always decreased by quantum effects in comparison with the Poisson value (this is always true for noninteracting electron systems, and remains true for interacting electrons in the elastic dephasing limit considered in this paper). A standard measure of the sub-Poissonian shot noise is the Fano factor defined as

$$F \equiv \frac{S_{\rm shot}}{2e\langle I\rangle} \equiv \frac{S_{\rm shot}}{S_{\rm poisson}} = \frac{{\rm Tr}\, T_{\rm tot}(1-T_{\rm tot})}{{\rm Tr}\, T_{\rm tot}} = \frac{\sum_j T_j(1-T_j)}{\sum_j T_j}, \tag{23}$$

where T_j are the eigenvalues of the total transmission matrix $T_{\rm tot}$. From Eq. (23), it can be inferred that the crossover from noise to noiseless transport regime can be best signaled by the emergence of perfectly transmitting eigenchannels in selected energy intervals of interest.

VI. NUMERICAL RESULTS

With the formalism considered so far, we evaluate the conductance and the Fano factor for quantum wires under different conditions of dephasing, magnetic field and Fermi energy. The comparison between the results in the absence and in the presence of magnetic fields is particularly interesting because it allows one to assert the robustness of the conductance quantization in the integer quantum Hall regime quantitatively, and to analyze the microscopic conditions that favor the dissipationless regime.

The study of the crossover between the noise and the noiseless regime is quite demanding, and requires not only the sound formal apparatus discussed in the previous sections but also the highest numerical accuracy. This can be achieved with the tools provided by the renormalization-decimation or other recursive techniques,[30–34] routinely developed in the formulation of the Keldysh nonequilibrium Green's function theory within the tight-binding framework. In particular, we refer to a paper[34] for technical details and procedures. Here, we briefly summarize the essential aspects of the dephasing model and choice of parameters for the quantum wires.

The continuous electronic gas system of the quantum wire is discretized on a square lattice of edge a, with a single orbital per site of energy E_0, and nearest-neighbor hopping parameter t. The open electronic wire is infinitely extended along the x direction and has width $W=(N-1)a$, where N is the number of chains. In the presence of a magnetic field in the positive z direction, described by the gauge vector potential $\mathbf{A}(\mathbf{r})=(-B\,y,0,0)$, the electron Hamiltonian of the clean system takes the form

$$H = E_0 \sum_{\rm mn} c^\dagger_{\rm mn} c_{\rm mn} + t \sum_{\rm mn} [c^\dagger_{\rm mn} c_{\rm mn+1} + c^\dagger_{\rm mn+1} c_{\rm mn}] + t \sum_{\rm mn} [e^{-i2\pi\alpha n} c^\dagger_{\rm mn} c_{m+1n} + e^{+i2\pi\alpha n} c^\dagger_{m+1n} c_{\rm mn}], \tag{24}$$

where $c^\dagger_{\rm mn}, c_{\rm mn}$ are creation and annihilation operators for electrons in the orbital at the site (ma,na). The Peierls phase is given by $\alpha=\Phi_p(B)/\Phi_0$ where $\Phi_p(B)=Ba^2$ is the magnetic flux through the elementary plaquette and $\Phi_0=hc/e$ is the flux quantum. For an ideal defect free wire, all the diagonal matrix elements are set equal to $E_0=-4t$.

Let us consider a model 200 nm wide quantum wire, and discretize it on a square grid with $N=150$ chains, i.e., $a \approx 1.342$ nm. The electron effective mass is taken $m^*=0.067m_e$ (typical of the GaAs-AlGaAs heterostructure), and the nearest-neighbor hopping parameter is thus $t \approx -424$ meV. The quantum wire is considered both in the absence and in the presence of perpendicular magnetic fields. In the case of a magnetic field $B=10$ T, the Peierls phase factor is $\alpha \approx 4.35\times10^{-3}$, the magnetic length is $l_0 \approx 8.1$ nm, and the magnetic energy is $\hbar\omega_c \approx 17.3$ meV. We consider four values for the coupling parameters, namely $\gamma=0,100,200,400$ meV. The range of the nonvanishing values of γ has been chosen so that the mobility of electron carriers, estimated from the change of resistance of the two-terminal device in the presence and in the absence of scattering, is in the typical range 10^4-10^5 cm^2 V^{-1} s^{-1} of the samples used in transport and magnetotransport measurements. As central disorder region we take a single column of sites in Figs. 2 and 3, two columns in Figs. 4 and 5, and five columns in Figs. 6 and 7. These models, corresponding to $M=1,2,5$ in Fig. 1, provide the exact quantitative description and intuitive understanding of the interplay of magnetotransport and dephasing effects, at a reasonable computational level. For the treatment of many-body effects active in longer multicolumn central devices, the numerical burden is correspondingly increased. For large size central regions, an avenue that could be addressed is to combine discussed concepts and procedures for phase randomizing processes with the lowest-order current-conserving expansion of the self-consistent Born approximation, so successful in the field of transport and dissipation in molecular electronics.[2,3]

We begin to discuss the numerical results in the case where the central disorder region is composed of a single column of sites, and in the absence of magnetic fields. In Fig. 2, we report the total conductance, the coherent and incoherent contributions, and the Fano factor as a function of energy in the absence of magnetic fields at various values of the coupling constant. The incoherent contribution increases in correspondence of the steps between plateaus, and remains small but still significant elsewhere. The total conductance never quantizes exactly to integer values, since backscattering is not suppressed. The curves reporting the Fano factor are even more revealing: The Fano factor is higher for energies near the thresholds of the steps, corresponding to the activation of a new conductive channel, while it decreases by 1 or 2 orders of magnitude for intermediate energies.

Figure 3 reports the results for the same 200 nm wide quantum wire threaded by a uniform magnetic field of 10 T.

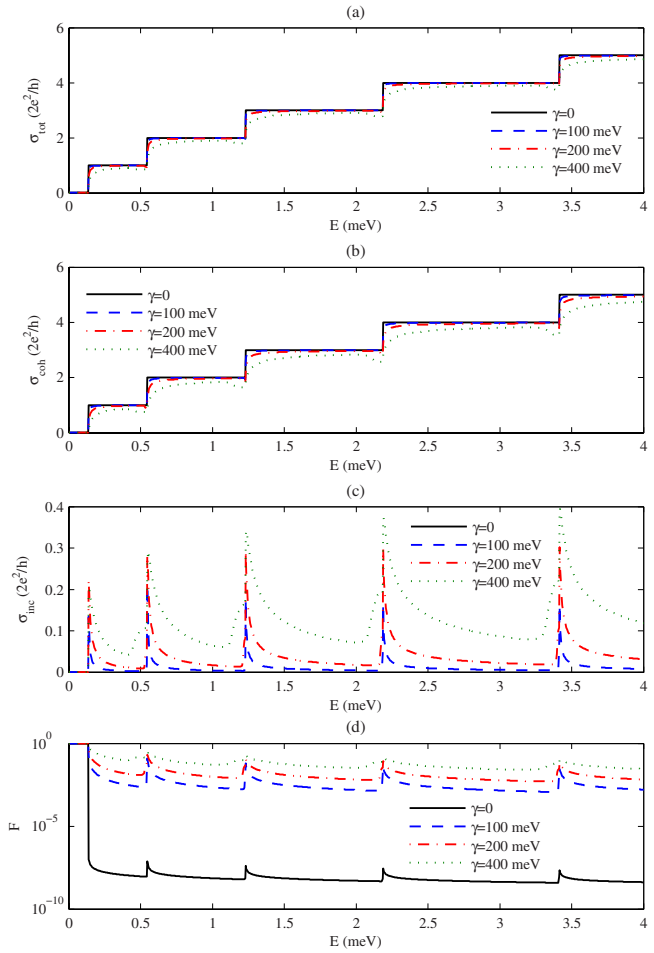

FIG. 2. (Color online) Total (a), coherent (b) and incoherent (c) differential conductance, and logarithmic value of the Fano factor (d) for 200 nm wide wire in the absence of magnetic fields, for $\gamma = 0, 100, 200, 400$ meV. In (a) and (b) the curves with increasing values of γ are (in general) smaller; in (c) and (d) the opposite occurs. The dephasing effects are active in a single column of the device. The current flow, characterized by noninteger values of the conductance and non-negligible noise, is dissipative at any energy.

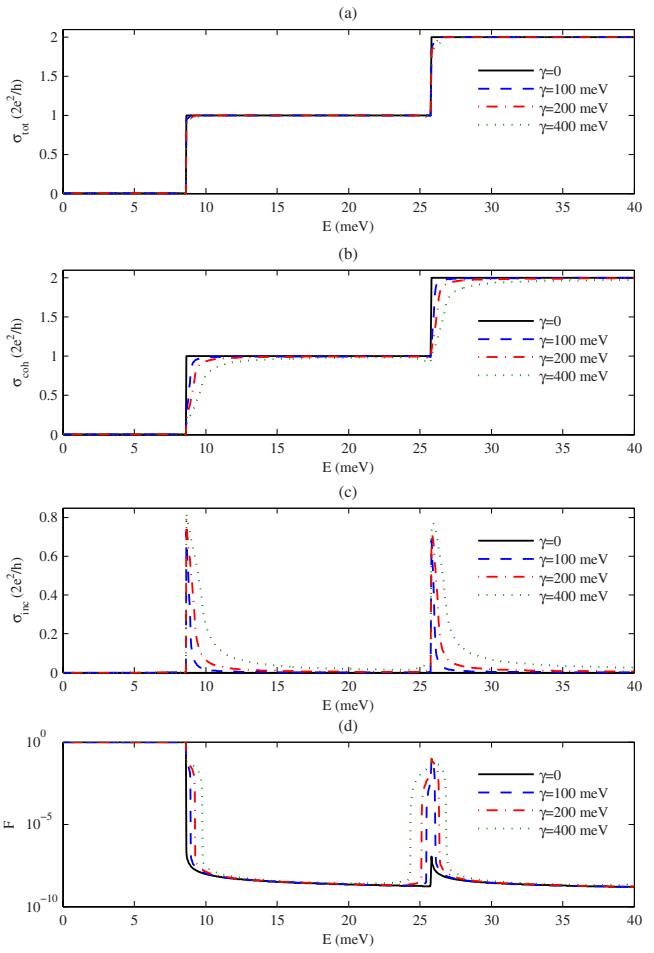

FIG. 3. (Color online) Total (a), coherent (b) and incoherent (c) differential conductance, and logarithmic value of the Fano factor (d) for 200 nm wide wire in the presence of a 10 T magnetic field, for $\gamma = 0, 100, 200, 400$ meV. In (a) and (b) the curves with increasing values of γ are (in general) smaller; in (c) and (d) the opposite occurs. The dephasing effects are active in a single column of the device. Energy regions where the current flow is characterized by integer values of the conductance and no noise alternate with energy regions characterized by shot noise and noninteger values of the conductance.

Similarly to the previous figure, the incoherent term is significant especially at and near the edges of the steps, while the coherent term prevails within the steps. This shows that scattering events remain active both in the presence and in the absence of magnetic fields. The quenching of scattering processes is neither produced by the magnetic field nor required for dissipationless current flow: The novelty introduced by the magnetic field in the quantum wire characterized by a width much larger than the magnetic length is the backscattering suppression of both coherent and incoherent components flowing in the edge conductive channels, at energies far from the bulk Landau levels. This entails, in these energy intervals, perfect quantization of the conductance and concomitant vanishing of shot noise, which decreases at least by 7 orders of magnitude in the calculations reported in Fig. 3. The interplay between bulk states and edge states in the quantum Hall regime[21] emerges with great evidence from the observed shot-noise suppression. At energies around the Landau levels, where bulk states and edge states coexist, the incoherent contribution exhibits a sharp increase, the conductance quantization is lost and shot noise accompanies the dissipative current flow.

The peculiar universal features, observed in the case of the minimal model of Fig. 3, remain robust spectacular features also in the case of multicolumn central devices. Figures 4 and 5 refer to the case that the central disorder region covers two columns, while Figs. 6 and 7 refer to the case that dephasing is active on five columns of the wire. In the absence of magnetic fields (Figs. 2, 4, and 6), with increasing length of the central device, it is seen that the incoherent contribution increases and tends to become comparable (or even to prevail in some energy regions) with respect to the coherent contribution. In the presence of magnetic fields (Figs. 3, 5, and 7), it is seen that the energy extension of the dissipative and dissipationless regions is parameter dependent. At the same time, the universal features of the dissipa-

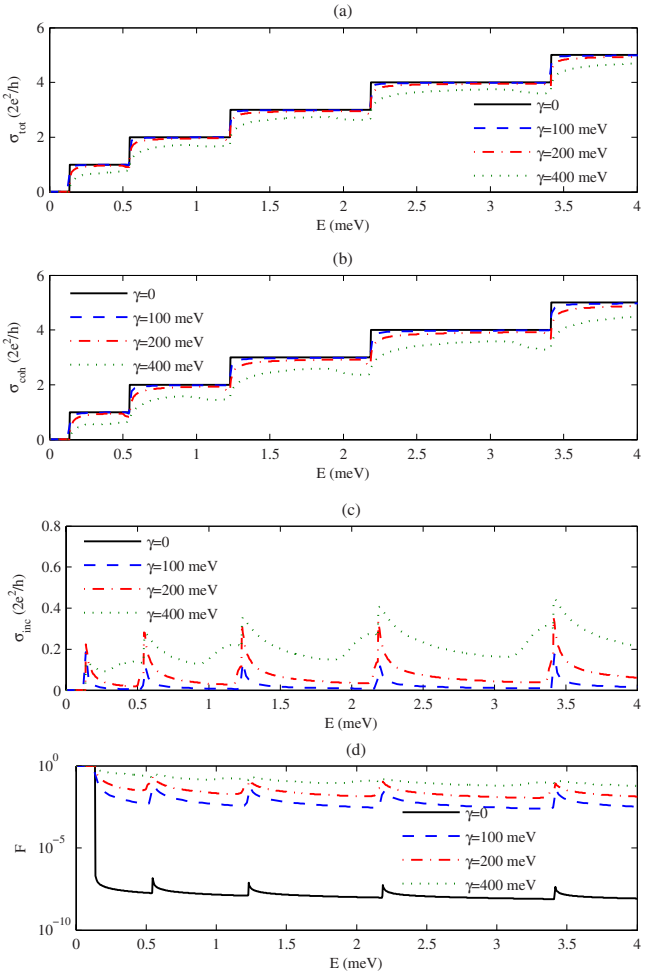

FIG. 4. (Color online) Total (a), coherent (b) and incoherent (c) differential conductance, and logarithmic value of the Fano factor (d) for 200 nm wide wire in the absence of magnetic fields, for $\gamma = 0, 100, 200, 400$ meV. In (a) and (b) the curves with increasing values of γ are (in general) smaller; in (c) and (d) the opposite occurs. The dephasing effects are active in two columns of the device. The current flow, characterized by noninteger values of the conductance and noise, is dissipative at any energy.

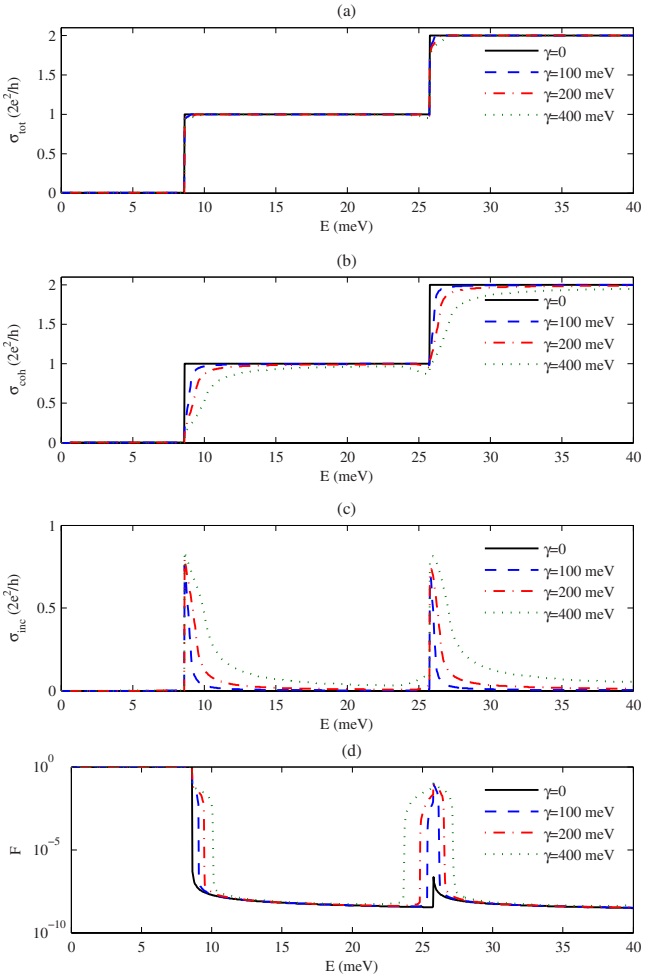

FIG. 5. (Color online) Total (a), coherent (b) and incoherent (c) differential conductance, and logarithmic value of the Fano factor (d) for 200 nm wide wire in the presence of a 10 T magnetic field, for $\gamma = 0, 100, 200, 400$ meV. In (a) and (b) the curves with increasing values of γ are (in general) smaller; in (c) and (d) the opposite occurs. The dephasing effects are active in two columns of the device. Energy regions where the current flow is characterized by integer values of the conductance and no noise alternate with energy regions characterized by shot noise and noninteger values of the conductance.

tionless regime (perfect integer quantization of conductance and perfect quenching of the current fluctuations) emerge with evidence, regardless of the length of the scattering region and of the strength of the many-body interactions.

VII. CONCLUSIONS

The many-body Keldysh formalism of quantum transport provides a reliable description of the dephasing effects on the electronic conductance and shot noise for quantum wires. In elaborating the self-consistent Born approximation to the many-body interactions, we have established some general results that go beyond the specific two-dimensional mesoscopic systems considered in this paper. In particular, we have shown that the electron conductance is naturally split into the sum of incoherent and coherent components, which correspond to carriers crossing the system with or without the assistance of scattering events. We have also demonstrated that, in the local models of dephasing, shot noise is always decreased in comparison with the Poisson value by quantum effects. For interacting electrons, the noise is controlled by the total transmission matrix, which is inclusive of coherent and incoherent components.

The high-accuracy numerical study of average current and current fluctuations is achieved by means of continued fraction expansion of the retarded and advanced propagators, and linear nonhomogeneous equations for the lesser and greater Green's functions. In the absence of magnetic fields and even in clean quantum wires, the dephasing effects are responsible for dissipative current flow, with nonquantized conductance values and finite shot noise. In quantum Hall wires in strong magnetic fields, we have observed both the dissipative regime and the dissipationless regime, with its striking universal aspects, plateau robustness and noiseless current flow.

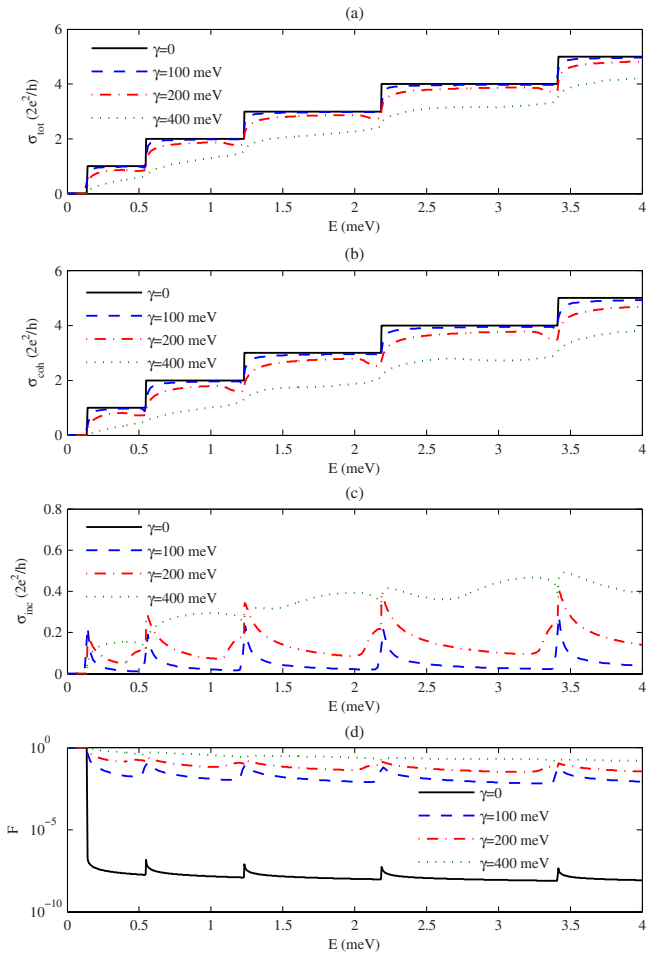

FIG. 6. (Color online) Total (a), coherent (b) and incoherent (c) differential conductance, and logarithmic value of the Fano factor (d) for 200 nm wide wire in the absence of magnetic fields, for $\gamma = 0, 100, 200, 400$ meV. In (a) and (b) the curves with increasing values of γ are (in general) smaller; in (c) and (d) the opposite occurs. The dephasing effects are active in five columns of the device. The current flow, characterized by noninteger values of the conductance and noise, is dissipative at any energy.

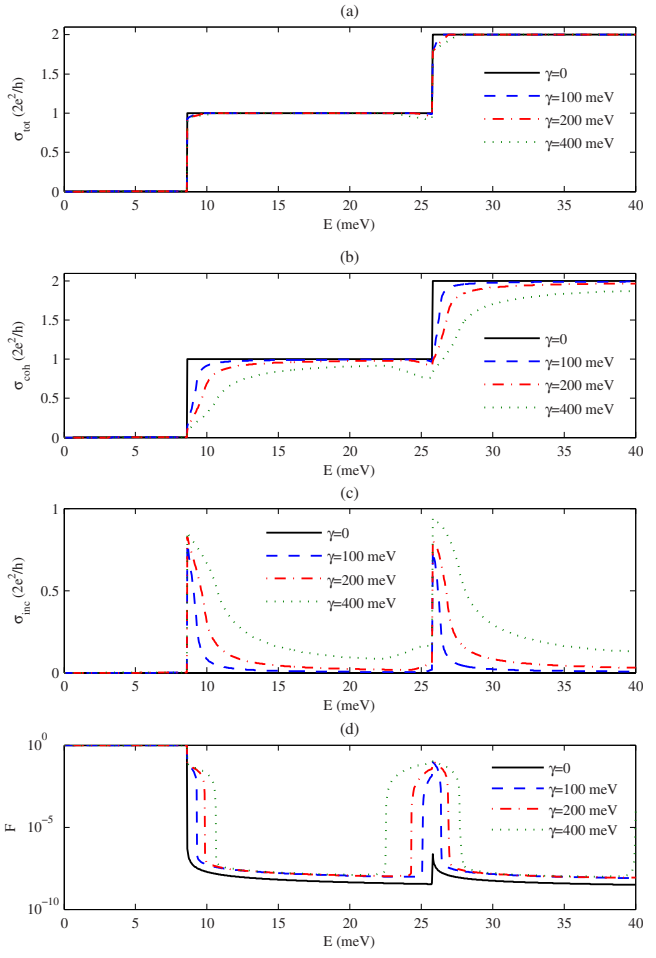

FIG. 7. (Color online) Total (a), coherent (b) and incoherent (c) differential conductance, and logarithmic value of the Fano factor (d) for 200 nm wide wire in the presence of a 10 T magnetic field, for $\gamma = 0, 100, 200, 400$ meV. In (a) and (b) the curves with increasing values of γ are (in general) smaller; in (c) and (d) the opposite occurs. The dephasing effects are active in five columns of the device. Energy regions where the current flow is characterized by integer values of the conductance and no noise alternate with energy regions characterized by shot noise and noninteger values of the conductance.

The present procedure for the investigation of dephasing effects, adaptable to other models of many-body interactions, could find application in the study of transport in other two-dimensional systems, including the rich phenomenology of spin-Hall transport and carbon-based devices.

ACKNOWLEDGMENTS

This work was partially supported by National Enterprise for nanoScience and nanoTechnology (NEST) and Scuola Normale Superiore of Pisa.

[1] T. Seideman, J. Phys.: Condens. Matter **15**, R521 (2003).
[2] T. Frederiksen, M. Paulsson, M. Brandbyge, and A. P. Jauho, Phys. Rev. B **75**, 205413 (2007).
[3] A. Pecchia, G. Romano, and A. Di Carlo, Phys. Rev. B **75**, 035401 (2007).
[4] J. K. Viljas, J. C. Cuevas, F. Pauly, and M. Häfner, Phys. Rev. B **72**, 245415 (2005).
[5] J.-C. Charlier, X. Blase, and S. Roche, Rev. Mod. Phys. **79**, 677 (2007).
[6] L. P. Zârbo and B. K. Nikolić, Europhys. Lett. **80**, 47001 (2007).
[7] L. Siddiqui, A. W. Ghosh, and S. Datta, Phys. Rev. B **76**, 085433 (2007).
[8] T. Stauber and N. M. R. Peres, J. Phys.: Condens. Matter **20**, 055002 (2008).

[9] A. Pecchia and A. Di Carlo, Rep. Prog. Phys. **67**, 1497 (2004).
[10] Y. A. Berlin, A. L. Burin, and M. A. Ratner, Chem. Phys. **275**, 61 (2002).
[11] A. Troisi and M. A. Ratner, Phys. Rev. B **72**, 033408 (2005).
[12] M. Galperin, A. Nitzan, and M. A. Ratner, Phys. Rev. B **75**, 155312 (2007).
[13] B. K. Nikolić, L. P. Zârbo, and S. Souma, Phys. Rev. B **73**, 075303 (2006).
[14] N. Samarth, in *Solid State Physics*, edited by H. Ehrenreich and F. Spaepen (Academic, San Diego, 2004), Vol. 58, p. 1.
[15] T. Ando, Phys. Rev. B **49**, 4679 (1994).
[16] F. Gagel and K. Maschke, Phys. Rev. B **54**, 13885 (1996).
[17] M. Büttiker, Phys. Rev. B **38**, 9375 (1988).
[18] G. Metalidis and P. Bruno, Phys. Rev. B **73**, 113308 (2006).
[19] A. Cresti, G. Grosso, and G. P. Parravicini, Phys. Rev. B **77**, 115408 (2008).
[20] K. v. Klitzing, G. Dorda, and M. Pepper, Phys. Rev. Lett. **45**, 494 (1980).
[21] D. Yoshioka, *The Quantum Hall Effect* (Springer, Berlin, 2002).
[22] D. K. Ferry and S. M. Goodnick, *Transport in Nanostructures* (Cambridge University Press, Cambridge, England, 1997).
[23] R. Lake, G. Klimeck, R. C. Browen, and D. Jovanovic, J. Appl. Phys. **81**, 7845 (1997).
[24] S. Datta, *Quantum Transport: Atom to Transistor* (Cambridge University Press, Cambridge, England, 2005).
[25] M. Galperin, M. A. Ratner, and A. Nitzan, J. Phys.: Condens. Matter **19**, 103201 (2007).
[26] A. Wacker and Ben Yu-Kuang Hu, Phys. Rev. B **60**, 16039 (1999).
[27] Z. Bihary and M. A. Ratner, Phys. Rev. B **72**, 115439 (2005).
[28] R. Golizadeh-Mojarad and S. Datta, Phys. Rev. B **75**, 081301(R) (2007).
[29] A. Cresti, G. Grosso, and G. Pastori Parravicini, J. Phys.: Condens. Matter **18**, 10059 (2006).
[30] D. W. Bullet, R. Haydock, V. Heine, and M. J. Kelly, in *Solid State Physics*, edited by H. Ehrenreich, F. Seitz, and D. Turnbull (Academic, New York, 1980), Vol. 35, p. 1.
[31] G. Grosso and G. Pastori Parravicini, *Solid State Physics* (Academic, London, 2000).
[32] G. Metalidis and P. Bruno, Phys. Rev. B **72**, 235304 (2005).
[33] F. Triozon and S. Roche, Eur. Phys. J. B **46**, 427 (2005).
[34] A. Cresti, G. Grosso, and G. Pastori Parravicini, Eur. Phys. J. B **53**, 537 (2006).
[35] J. X. Zhu and A. V. Balatsky, Phys. Rev. B **67**, 165326 (2003).